Field-induced Dielectrophoresis and Phase Separation for Manipulating Particles in Microfluidics

D.J. Bennett[*], B. Khusid[**], C.D. James[***], P.C. Galambos[****], M. Okandan[*****], D. Jacqmin[******], A. Kumar[*******], Z. Qiu[********], and A. Acrivos[*********]

[*]New Jersey Institute of Technology, University Heights, Newark, NJ 07102 and Sandia National Laboratories, POB 5800, Albuquerque, NM 87185, djbenne@sandia.gov
[**]New Jersey Institute of Technology, University Heights, Newark, NJ 07102, khusid@adm.njit.edu
[***]Sandia National Laboratories, POB 5800, Albuquerque, NM 87185, cdjame@sandia.gov
[****]Sandia National Laboratories, POB 5800, Albuquerque, NM 87185, pcgalam@sandia.gov
[*****]Sandia National Laboratories, POB 5800, Albuquerque, NM 87185, mokanda@sandia.gov
[******]NASA Glenn Research Center, Cleveland, OH 44135, fsdavid@tess.lerc.nasa.gov
[*******]City College of New York, 140th St., New York, NY 10031, anil@levdec.engr.ccny.cuny.edu
[********]City College of New York, 140th St., New York, NY 10031, qiu@lisgi6.engr.ccny.cuny.edu
[*********]City College of New York, 140th St., New York, NY 10031, acrivos@scisun.sci.ccny.cuny.edu

ABSTRACT

We report observations of a new electric field- and shear-induced many-body phenomenon in the behavior of suspensions. Its origin is dielectrophoresis accompanied by the field-induced phase separation. As a result, a suspension undergoes a field-driven phase separation leading to the formation of a distinct boundary between regions enriched with and depleted of particles. The theoretical predictions are consistent with experimental data even though the model contains no fitting parameters. It is demonstrated that the field-induced dielectrophoresis accompanied by the phase separation provides a new method for concentrating particles in focused regions and for separating biological and non-biological materials, a critical step in the development of miniaturizing biological assays.

Keywords: dielectrophoresis, field-induced phase separation, concentrating particles, separation of biological and non-biological materials

Compared to other available methods, ac dielectrophoresis is particularly well-suited for the manipulation of minute particles in microfluidics [1]. The ac dielectrophoretic force acting on a sphere immersed in a liquid is [2]

$$\mathbf{F}_{\mathrm{dep}} = \frac{3}{2}\varepsilon_0\varepsilon_f v_p \,\mathrm{Re}[\beta(\omega)]\nabla\langle \mathbf{E}^2\rangle \qquad (1)$$

where v_p is the particle volume, ε_0 is the vacuum permittivity, ε_f is the dielectric constant of the liquid, $\mathrm{Re}(\beta)$ is the real part of the relative particle polarization at the field frequency β, and $\langle\ \rangle$ denotes time averaging over the field oscillation. Depending on the sign of $\mathrm{Re}(\beta)$, the particle moves toward the regions of high field strength (positive dielectrophoresis) or low field strength (negative dielectrophoresis). The concepts currently favored for the design and operation of dielectrophoretic micro-devices adopt the approach used for macro-scale electric filters [3]. This strategy considers the trend of the field-induced particle motions by computing the spatial distribution of the field strength over a channel as if it were filled only with a liquid and then evaluating the direction of the dielectrophoretic force, Eq. (1), exerted on a single particle placed in the liquid. However, the exposure of suspended particles to a field generates not only the dielectrophoretic force acting on each of these particles, but also the dipolar interactions of the particles due to their polarization. Furthermore, the field-driven motion of the particles is accompanied by their hydrodynamic interactions. These long-range electrical and hydrodynamic interparticle interactions are entirely neglected in analyzing the performance of currently used micro-fluidic devices.

In [4-6], we demonstrated that a single-particle model which only takes into account the dielectrophoretic force, Eq. (1), the Stokes drag force, and the gravity force acting on a particle predicts fairly well the rate of the field-driven particle redistribution for dilute suspensions containing ~ 0.1% (v/v) but does not predict the aggregation pattern formed by these particles. Furthermore, the presence of the interparticle dipole-dipole interactions was found to impose a lower bound on the scale of microelectrode arrays for the precise positioning of positively polarized particles in selected locations of a dielectrophoretic micro-channel even for ~0.1% (v/v) suspensions [7]. Now we report observations of dielectrophoresis accompanied by a field-induced phase separation whose origin is the interparticle electric interactions. As a result, a suspension of negatively

polarized particles undergoes a field-driven phase separation leading to the formation of a distinct boundary between regions enriched with and depleted of particles.

Microfluidic devices for experiments were fabricated in Sandia National Laboratories Microelectronics Development LAB using Sandia's SwIFTTM (Surface micromachining with Integrated microFluidics Technology) process [8, 9] for producing highly-integrated monolithic multilayer structures. The fluidic channels, fabricated using single 6 inch Si wafers, are 40 μm wide, 6 μm high, and 570μm long and contain 6 μm wide p-doped polysilicon traces, with each trace being split into two electrically-connected electrodes located on the ceiling and the floor of the fluidic channel and arranged perpendicular to the flow (Fig. 1) [10]. Access ports to the channels were fabricated using a two step Bosch-etch process which consists of a counter-bore backside etch partly into the Si substrate, followed by a through-wafer etch to the channels on the front surface of the substrate. The suspension was delivered into the channel at a flow rate ranging from 0.24 pL/s to 9.6 pL/s. The electrodes were energized with a sinusoidal wave, 10 V peak-to-peak (ptp) and 15-30 MHz while the silicon substrate was grounded. These electrodes act like "dielectrophoretic gates" [according to Eq. (1)], that control the motion of polarized particles flowing through the channel. The suspensions were prepared by dispersing 1μm polystyrene spherical beads (1.05 g/cm^3, Duke Scientific Co.) in deionized (DI) water. Following [4, 5], the bead polarizability, $\beta \cong -0.45 - 0.27i$ for 10-30 MHz was calculated from the low-field measurements of the suspension complex dielectric permittivity. The photos presented in Fig. 1 show the time evolution of the particle distribution in a 0.1% (v/v)-suspension from which it is evident that the beads, experiencing negative dielectrophoresis, are repelled from the dielectrophoretic gate and accumulate in a region near the electrodes (Fig. 1). On account of compressive electric and shear stresses, the layer of these beads forms a round bolus with a distinct front between the regions enriched with and depleted of particles. The average particle concentration in the bolus was estimated [10] to run as high as 40-50% (v/v).

An electro-hydrodynamic model proposed for simulating the bolus formation [10] generalizes a thermodynamic theory [11-13] for a suspension subject to a spatially non-uniform ac field. This model encompasses the quasi-steady electrodynamic equations together with the momentum and continuity balance equations of the "mixture" model for a suspension, which are averaged over the field oscillations. The suspension is viewed as an effective Newtonian fluid the viscosity which varies with the particle concentration according to the Leighton-Acrivos expression. The bulk electric force exerted on a suspension, and the particle velocity relative to the suspending fluid are expressed in terms of the chemical potential of the particles [11-13]. Depicted in Fig. 2 is the simulation of the time evolution of the particle distribution using the data for water, for the particle properties, and for the channel dimensions presented above. As can be seen, the particles, which accumulate in the region close to the microelectrodes, undergo a field-induced phase separation and form two concentrated layers near the channel top and bottom (Fig. 2). The theoretical predictions for the bolus growth, for the particle concentration in the bolus, and the fact that particles travel around the circumference of the bolus and are then drawn into the bolus side closest to the electrode, are consistent with the observations (Fig. 1). In line with the experiments, the simulations indicated that our experimental conditions lie in the transition region between the formation of one bolus located near the channel centerline and two boluses attached to the channel side walls. For example, a slight change (~8%) in the voltage distribution along the microelectrode leads to the appearance of two boluses [Fig. 2(d, h)].

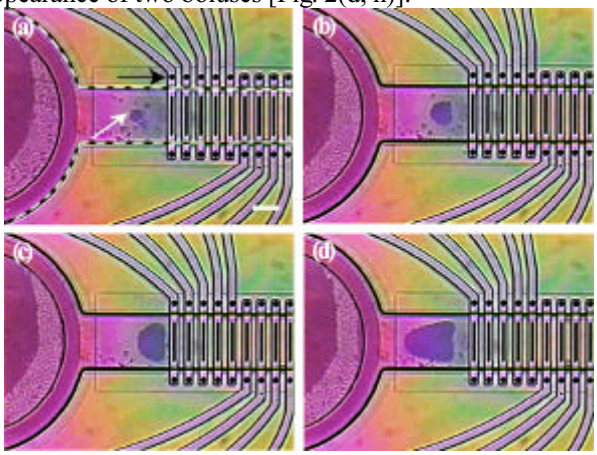

Figure 1. Dielectrophoresis (10V ptp, 30 MHz) of beads accompanied by a phase separation (white arrow). The dashed lines denote the outline of the fluidic channel, and the black arrow indicates the energized electrode. The dark regions on the polysilicon traces indicate the places where the ceiling electrodes are in direct contact with the fluid. The time is (a) 10s, (b) 70s, (c) 120s, and (d) 180s. The flow is from left to right. Scale bar = 20 μm [10].

The photo presented in Fig. 3 illustrates the dielectrophoretic separation of a heterogeneous mixture of polystyrene beads and heat-killed bacterial cells (Staphylococcus aureus; Molecular Probes) dispersed in DI water. The beads, experiencing negative dielectrophoresis, form two boluses adjacent to the channel walls [similar to the simulation results shown in Fig. 2 (d, h)]; whereas the cells, which are more polarizable than DI water at this frequency, experience positive dielectrophoresis and are collected on the electrode. The complete separation of the continuously flowing cell-bead mixture was achieved by cycling the activation of the electrode off and on. During the off phase, the cells and particles which were dielectrophoretically separated during the on phase, maintained their spatial separation and were carried along the channel to the outlet port, but, before the beads had reached the edge of the leading electrode, the field was turned back on, thereby repelling the beads again (Fig. 3) to

a distance ~ 20 μm from the electrode edge. In contrast, the cells which had not been collected on the electrode continued moving with the flow towards the outlet port of the device.

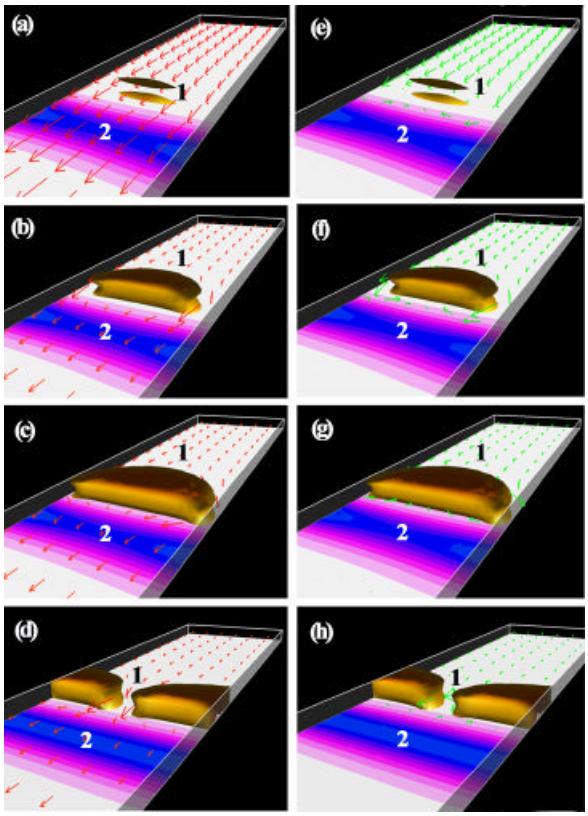

Figure 2. Numerical simulations of the concentration contours (1) for the 0.1 % (v/v)-suspension, 8.64 pL/s, 10 V ptp. In the panels, the fluid flow is from the upper right-hand corner to the lower left-hand corner. The color band (2) indicates the variation of E^2 (in kV^2/cm^2) along the channel bottom (white for up to 1.3, pink for 1.3-2.7, and blue for 10.6-11.9), whose maximum is located near the first electrode (Fig. 1). Time is (a, e) 10s, (b, f) 70s, (c, g) 180s, and (d, h) 120s. The computed values for c_{max} in the bolus [in % (v/v)] are (a) 8.73, (b) 45.4, and (c) 56.4, and (d) 54.1. In (a) to (d), the red arrows show the relative magnitude of the flow velocity [v_{max} (in μm/s) = (for t=0) 36, (a) 49.8, (b) 106.3, (c) 110.4, and (d) 139.9]. In (e) to (h), the green arrows show the relative magnitude of the particle velocity, $v_{p,max}$ (in μm/s) = (for t=0) 36, (e) 45.2, (f) 78.8, (g) 151.4, and (h) 171.6] [10].

To test theoretical predictions quantitatively, experiments were conducted [14] on 5%–15 %(v/v) suspensions of neutrally buoyant spherical (average diameter of 87 μm) polyalphaolefin particles (AVEKA, Woodbury, MN) suspended in corn oil ($0.92 g/cm^3$, 59.7 cp at 23^0C) which exhibit negative dielectrophoresis. Following [4, 5], the particle polarizability was calculated from the low-field measurements of the suspension complex dielectric permittivity: $\mathrm{Re}(\beta) \cong -0.15$ was found to equal, approximately, -0.15 for 0.1- 3.5 kHz, whereas $\mathrm{Im}(\beta)$ was found to decrease rapidly with frequency from $1.8 \cdot 10^{-3}$ for 0.1 kHz to less than $2 \cdot 10^{-4}$ for frequencies greater than 1 kHz. The experiments were performed in a horizontal parallel-plate chamber (6 cm wide, 12 cm long, and 3 mm high). The bottom of the chamber was equipped with electrodes (1.6 mm wide) which were embedded into groves at 2 mm intervals (Fig. 4) and were alternately connected to the high voltage and to the ground. The top of the chamber, consisting of a transparent glass coated with a conducting layer of indium tin oxide, was grounded. Under these conditions, the field configuration consists of two high-strength regions near the electrode edges and a wide low-strength region above the center of the grounded electrode near the channel midplane.

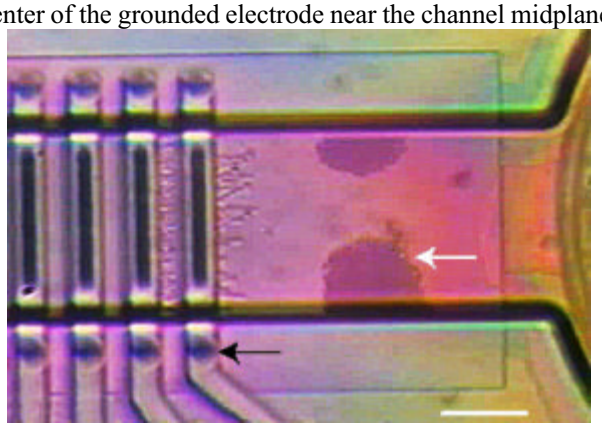

Figure 3. Dielectrophoretic (10V ptp, 15 MHz) separation of bacterial cells and beads. The cells adhere to the energized electrode (black arrow) while the beads experience negative dielectrophoresis accompanied by a phase separation (white arrow). The flow is from right to left. Scale bar = 20 μm [10].

The photos in Fig. 4 show the field-driven time evolution of the particles (seen as white spots in the photos) in the 10%(v/v)-suspension. After about 150 s a distinct front between the suspension and the suspending fluid containing very few particles [Fig. 4(d)] formed along the channel. As time progressed, the front slowly moved away from the high field regions and the particles became progressively confined to a thin column above the grounded electrode. Note that the same configuration of an electric field does not lead to the front formation in dilute suspensions, ~0.01%-0.2% (v/v) [4].

Simulations were conducted using the data of fluid and particle properties and the channel dimensions presented above. The theory predicts that the use of the characteristic time for dielectrophoresis τ_d, Eq. (2), [4, 5] makes it possible to combine the data on the time dependence of the front position for different voltages and frequencies (Fig. 5) into one band for $t/\tau_d \le 20$. Here

$$\tau_d = \frac{3d^4\eta_f}{a^2\varepsilon_0\varepsilon_f|\mathrm{Re}(\beta)|V_{rms}^2}, \qquad (2)$$

where η_f is the viscosity of the suspending fluid, d is the electrode width, a is the particle radius, and V_{rms} is the root mean square of the applied ac voltage. As can be seen from Fig. 5 (b), the simulation results are in a reasonable agreement with the experimental data.

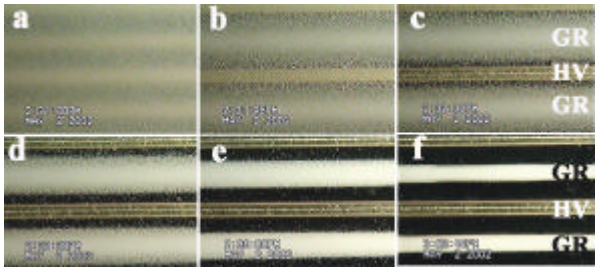

Figure 4. The particle distribution in a suspension with 10%(v/v) particle concentration (a) before and (b)-(f) following the application of a field 5kVrms, 100Hz at (b) 45s, (c) 90s, (d) 150s, (e) 300s, and (f) final state, ~39min. The electrode width is 1.6mm. HV and GR refer to high-voltage and grounded electrodes respectively [14].

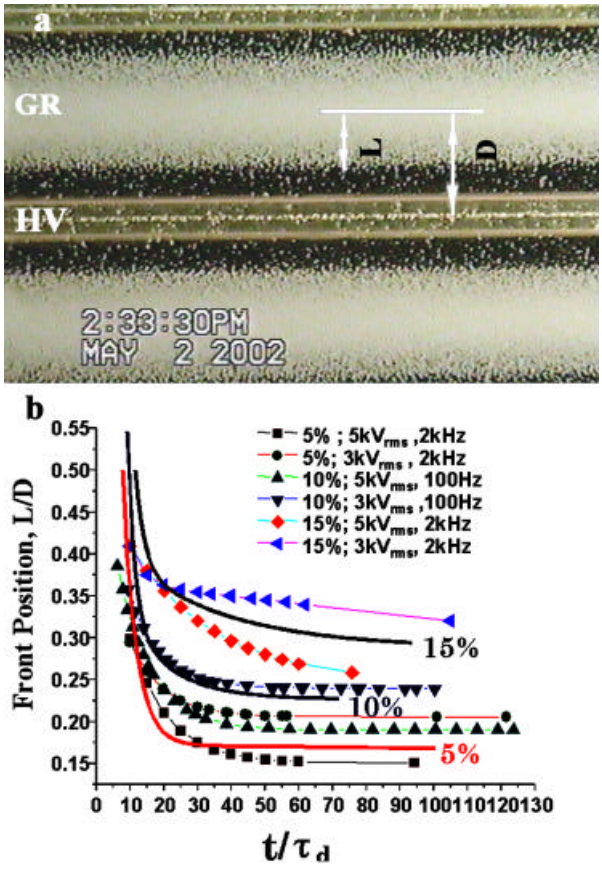

Figure 5. (a) The photo illustrates how the front location was measured; HV and GR refer to the high-voltage and grounded electrode respectively. (b) The experimental data (symbols) and computational results (solid lines) for 5%, 10%, and 15% (v/v) suspensions [14].

In conclusion, we demonstrated that dielectrophoresis accompanied by a field-induced phase transition provides a powerful method for strongly concentrating particles and for separating biological and non-biological particles. In particular, substances less polarizable than water (nearly all inorganic materials) can be removed from aqueous solutions. The predictions of the proposed electro-hydrodynamic model are consistent with the experiments even though the model contains no fitting parameters.

The work was supported, in part, by grants from the NASA, NAG3-2698 (B.K., Z.Q., and A.A), and from the DARPA through the Bioflips/Simbiosys Program, Mission Research Corporation/DARPA Contract # DAAH01-02-C-R083 (B.K.). D.B. thanks Sandia's MESA Institute and the NSF MAGNET/SEM program for support. The properties of polystyrene beads were measured by Len Duda (Sandia). The properties of polyalphaolefin particles were measured at the NJIT W.M. Keck Foundation Laboratory. Sandia is a multiprogram laboratory operated by Sandia Corporation, a Lockheed Martin Company, for the U.S. DOE under contract DE-ACO4-94-AL85000.

REFERENCES

[1] P.R.C. Gascoyne and J. Vykoukal, Electrophoresis 23, 1973 (2002).

[2] T.B. Jones, "Electromechanics of Particles," Cambridge University Press, 1995.

[3] "Handbook of Electrostatic Processes," Eds. J.-S. Chang, A.J. Kelly, and J.M. Crowley, Marcel Dekker, 1995.

[4] A. Dussaud, B. Khusid, and A. Acrivos, J. Appl. Phys., 88, 5463 (2000).

[5] Z. Qiu, N. Markarian, B. Khusid, and A. Acrivos, J. Appl. Phys., 92, 2829 (2002).

[6] N. Markarian, M. Yeksel, B. Khusid, K. Farmer, and A. Acrivos, J. Appl. Phys., 94, 4160 (2003).

[7] N. Markarian, M. Yeksel, B. Khusid, K. Farmer, and A. Acrivos, Appl. Phys. Lett., 82, 4839 (2003).

[8] M. Okandan, P. Galambos, S. Mani, and J. Jakubczak, "Proceedings of SPIE," 4560, 133 (2001).

[9] M. Okandan, P. Galambos, S. Mani, and J. Jakubczak, "Micro Total Analysis Systems 2001," 305-306.

[10] D.J. Bennett, B. Khusid, C.D. James, P.C. Galambos, M. Okandan, D. Jacqmin, and A. Acrivos, Appl. Phys. Lett., 83, 4866 (2003).

[11] B. Khusid and A. Acrivos, Phys. Rev. E, 52, 1669 (1995).

[12] B. Khusid and A. Acrivos, Phys. Rev. E 60, 3015 (1999).

[13] B. Khusid and A. Acrivos, Phys. Rev. E 54, 5428 (1996).

[14] A. Kumar, Z. Qiu, A. Acrivos, B. Khusid, and D. Jacqmin, Phys. Rev. E 69, (2004) (*accepted*)